WPP-Domain Proteins Mimic the Activity of the HSC70-1 Chaperone in Preventing Mistargeting of RanGAP1-Anchoring Protein WIT1[1][C][W][OA]

Jelena Brkljacic[2], Qiao Zhao[2,3], and Iris Meier*

Department of Plant Cellular and Molecular Biology, Plant Biotechnology Center, The Ohio State University, Columbus, Ohio 43210

Arabidopsis (*Arabidopsis thaliana*) tryptophan-proline-proline (WPP)-domain proteins, WPP1 and WPP2, are plant-unique, nuclear envelope-associated proteins of unknown function. They have sequence similarity to the nuclear envelope-targeting domain of plant RanGAP1, the GTPase activating protein of the small GTPase Ran. WPP domain-interacting tail-anchored protein 1 (WIT1) and WIT2 are two Arabidopsis proteins containing a coiled-coil domain and a C-terminal predicted transmembrane domain. They are required for RanGAP1 association with the nuclear envelope in root tips. Here, we show that WIT1 also binds WPP1 and WPP2 in planta, we identify the chaperone heat shock cognate protein 70-1 (HSC70-1) as in vivo interaction partner of WPP1 and WPP2, and we show that HSC70-1 interacts in planta with WIT1. WIT1 and green fluorescent protein (GFP)-WIT1 are targeted to the nuclear envelope in Arabidopsis. In contrast, GFP-WIT1 forms large cytoplasmic aggregates when overexpressed transiently in *Nicotiana benthamiana* leaf epidermis cells. Coexpression of HSC70-1 significantly reduces GFP-WIT1 aggregation and permits association of most GFP-WIT1 with the nuclear envelope. Significantly, WPP1 and WPP2 show the same activity. A WPP1 mutant with reduced affinity for GFP-WIT1 fails to decrease its aggregation. While the WPP-domain proteins act on a region of WIT1 containing the coiled-coil domain, HSC70-1 additionally acts on the C-terminal transmembrane domain. Taken together, our data suggest that both HSC70-1 and the WPP-domain proteins play a role in facilitating WIT1 nuclear envelope targeting, which is, to our knowledge, the first described in planta activity for the WPP-domain proteins.

The cytoplasmic Ran GTPase activating protein RanGAP is critical to establishing a functional RanGTP/RanGDP gradient across the nuclear envelope (NE) and is associated with the outer surface of the NE in metazoan and higher plant cells (Matunis et al., 1996; Rose and Meier, 2001). Plant RanGAP1 association with the NE requires a plant-specific targeting domain, named the Trp-Pro-Pro (WPP) domain (Rose and Meier, 2001). Arabidopsis (*Arabidopsis thaliana*) WPP1 and WPP2 are small (155- and 180-amino-acid residues, respectively) plant-unique proteins of unknown function, which are similar to the WPP domain of RanGAP proteins. WPP1 and WPP2 are located in the cytoplasm, with a concentration at the NE (Patel et al., 2004). They are characterized by a 104-amino-acid-long WPP domain, predicted to consist of a β-strand and three α-helices and shown to be sufficient for NE targeting (Patel et al., 2004). They are also associated with cytoplasmic speckles most likely representing Golgi (Patel et al., 2005). Reduced expression of the WPP protein family causes decreased mitotic activity in roots of Arabidopsis, resulting in shortening of primary roots and decreased number of lateral roots (Patel et al., 2004). RanGAP1 association with the NE in the Arabidopsis root tip requires two families of NE-localized, plant-specific, WPP domain-interacting proteins (WPP domain-interacting protein [WIP] and WPP domain-interacting tail-anchored protein [WIT] families) that are characterized by the presence of a coiled-coil domain and a C-terminal predicted transmembrane domain (TMD; Xu et al., 2007; Zhao et al., 2008). Based on sequence analysis, both the WIP and WIT protein family were classified as putative tail-anchored (TA) proteins, proteins that associate with membranes posttranslationally (Borgese et al., 2003).

The heat shock protein 70 family (HSP70) contains both heat-inducible and constitutively expressed members, called heat shock cognate proteins (HSC70). HSC70 chaperones assist in folding newly synthesized proteins (Bukau and Horwich, 1998), are involved in posttranslational translocation of secretory proteins across endoplasmic reticulum (ER) and mitochondrial

[1] This work was supported by the National Science Foundation (to I.M.).

[2] These authors contributed equally to the article.

[3] Present address: Samuel Roberts Noble Foundation, Ardmore, OK 73401.

* Corresponding author; e-mail meier.56@osu.edu.

The author responsible for distribution of materials integral to the findings presented in this article in accordance with the policy described in the Instructions for Authors (www.plantphysiol.org) is: Iris Meier (meier.56@osu.edu).

[C] Some figures in this article are displayed in color online but in black and white in the print edition.

[W] The online version of this article contains Web-only data.

[OA] Open access articles can be viewed online without a subscription.

www.plantphysiol.org/cgi/doi/10.1104/pp.109.143404

membranes (Chirico et al., 1988; Deshaies et al., 1988), prevent irreversible aggregation of their substrates (Ngosuwan et al., 2003), and facilitate degradation of misfolded proteins (Meacham et al., 2001). Recently, mammalian HSC70 has also been implied in assisting the membrane insertion of a subset of TA proteins (Abell et al., 2007).

The Arabidopsis genome encodes five different cytosolic HSP70s, three of which are expressed constitutively (*HSC70-1*, *HSC70-2*, and *HSC70-3*). While expressed in all organs, *Hsc70-1* and *Hsc70-2* expression levels are highest in leaves and *Hsc70-3* in leaves and roots. All three genes can be further induced by heat shock and cold stress (Sung et al., 2001). Constitutive overexpression of Arabidopsis *Hsc70-1* in transgenic plants leads to changes in growth and development, increases thermotolerance (Sung and Guy, 2003), and decreases the plant's ability to respond to pathogen attack (Noel et al., 2007). Recently, specific interactions of HSC70-1 with SGT1 (for Suppressor of G2 allele of *skp1*; Noel et al., 2007) and HSC70-3 with turnip mosaic virus RNA-dependent RNA polymerase (Dufresne et al., 2008) were identified, suggesting a role of HSC70 in viral replication and pathogenesis. Both HSC70-1 and HSC70-3 can be detected in the nuclei and the cytoplasm of *Nicotiana benthamiana* epidermal cells (Noel et al., 2007; Dufresne et al., 2008).

Here, we identified Arabidopsis HSC70-1 as an in vivo interaction partner of WPP1 and WPP2 and demonstrated that HSC70-1 associates with WIT1. Using transient expression in *N. benthamiana*, we show that when expressed at a high level, WIT1 accumulates in large fluorescent bodies in the cytoplasm that may represent aggregates. Upon coexpression in the same system, WPP1, WPP2, and HSC70-1 are all able to prevent the aggregation of overexpressed WIT1 and enable WIT1 association with the NE. While WPP-domain proteins act on a region of WIT1 containing the coiled-coil domain, HSC70-1 additionally acts on the C-terminal TMD. We propose that WPP1 and WPP2 play a chaperone-like role reflected in preventing the aggregation of the coiled-coil region of WIT1 and possibly other coiled-coil TA-type proteins, either in conjunction or independently of HSC70-type chaperones.

RESULTS

Identification of in Vivo WPP1 and WPP2 Complexes Containing HSC70-1 and HSC70-3

To identify proteins interacting with WPP1 and WPP2 in Arabidopsis, transgenic plants were made that express either WPP1 or WPP2 fused to a tandem affinity purification tag (Rohila et al., 2004). After tandem affinity purification, SDS-PAGE, and silver staining, the excised bands were subjected to mass spectrometry analysis. Five peptides corresponding to Arabidopsis cytosolic/nuclear HSC70 were identified in an 85-kD band of the TAP-WPP2 pull-down fraction. Similarly, four peptides belonging to the same HSC70 group of proteins, coming from an 85-kD band of the TAP-WPP1 pull-down fraction, were recognized (Supplemental Tables S1 and S2). The Arabidopsis genome encodes five different cytosolic/nuclear HSP70 genes, three of which are expressed constitutively (*HSC*70-1, *HSC*70-2, and *HSC*70-3; Sung et al., 2001). Sequences of several identified peptides do not allow identification of a specific HSP70, due to a high sequence similarity among different family members. However, some of the peptides unequivocally identified HSC70-1 (At5g02500) and HSC70-3 (At3g09440; Supplemental Tables S1 and S2). To confirm the interactions between WPP1, WPP2, HSC70-1, and HSC70-3, the corresponding cDNAs were cloned and HA-tagged proteins were coexpressed with GFP-tagged proteins by agroinfiltration in *N. benthamiana*. Figure 1A shows that WPP1 bound both HSC70-1 and HSC70-3, while WPP2 bound HSC70-1 but not HSC70-3 in this assay.

Two coiled-coil proteins WIT1 and WIT2 had been previously identified as in vivo WPP1 and WPP2 interactors from the same tandem affinity purification fractions (Zhao et al., 2008). Figure 1B shows that WPP1-WIT1 and WPP2-WIT1 interactions occur after agroinfiltration in *N. benthamiana*. Interactions between WPP-domain proteins and endogenous WIT1 or endogenous HSC70 were subsequently tested in transgenic Arabidopsis plants expressing either WPP1-GFP or WPP2-GFP under the control of their own promoters. In these lines, WPP1-GFP and WPP2-GFP are associated with the NE, Golgi-like speckles, and a meshwork-like structure that most likely represents ER, similar to the published 35S-driven fusions (Patel et al., 2004; data not shown). Figure 1C shows that WPP1 and WPP2 coimmunoprecitipate endogenous WIT1 and endogenous HSC70. Although the anti-HSC70 antibody recognizes all cytosolic forms of HSP70 (Zhang and Guy, 2005), this pool consists mostly of the constitutively expressed HSC70-1, HSC70-2, and HSC70-3 isoforms (Sung et al., 2001), thus likely representing the isoforms coimmunoprecipitated by WPP1 and WPP2.

Overexpressed WIT1 Forms ER-Associated Aggregates in the Cytoplasm

In agreement with the role in anchoring RanGAP1 to the NE, both endogenous WIT1 and GFP-WIT1 are targeted to the NE in Arabidopsis (Zhao et al., 2008; Fig. 2A). However, the attempts to localize GFP-WIT1 driven by the 35S promoter in different transient transformation systems repeatedly showed that overexpressed GFP-WIT1 forms large aggregate-like fluorescent bodies in the cytoplasm (called aggregates from here on). The aggregates occurred when GFP-WIT1 was expressed in protoplasts derived from an *N. benthamiana* cell culture or from Arabidopsis leaf mesophyll cells and in agroinfiltrated *N. benthamiana*

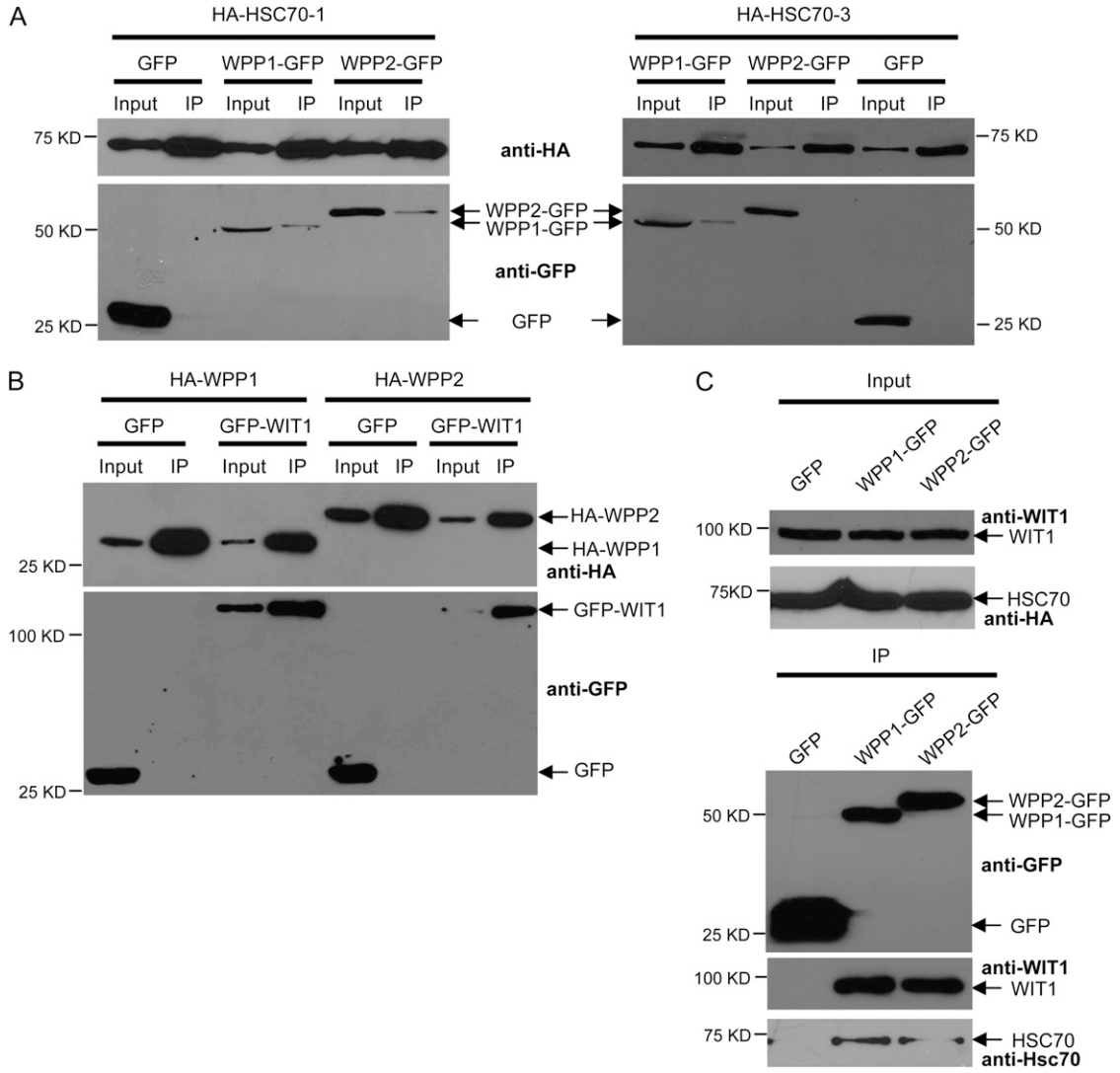

Figure 1. WPP domain proteins WPP1 and WPP2 interact with both WIT1 and HSC70 in vivo. A, HA-HSC70-1 was coexpressed with either GFP, WPP1-GFP, or WPP2-GFP (left); HA-HSC70-3 was coexpressed with either GFP, WPP1-GFP, or WPP2-GFP (right) in *N. benthamiana*. Immunoprecipitation was performed using the anti-HA antibody, and coimmunoprecipitated proteins were detected with the anti-GFP antibody. p19 was present in all *N. benthamiana* infiltrations. B, HA-WPP1 or HA-WPP2 was coexpressed with either GFP or GFP-WIT1 in *N. benthamiana*. Immunoprecipitation was performed using the anti-HA antibody, and coimmunoprecipitated proteins were detected with the anti-GFP antibody. p19 was present in all *N. benthamiana* infiltrations. C, Samples immunoprecipitated from 35S:GFP, WPP1:WPP1-GFP, and WPP2:WPP2-GFP transgenic lines using the anti-GFP antibody (top) were probed with the anti-WIT1 (middle) or the anti-Hsc70 antibody (bottom). IP, Immunoprecipitate.

leaves, when the strong silencing suppressor p19 was coinfiltrated (Fig. 2, B and C; Supplemental Fig. S1A). No obvious underlying structure, such as membrane whorls, could be observed within the aggregates, at the level of resolution of confocal microscopy (Supplemental Fig. S2). In the absence of p19, association of WIT1 with the NE could be detected (Supplemental Fig. S3), indicating that the aggregates were based on the high level of protein expression in the presence of p19 (Fig. 2C, left). Consistently, when the expression level of GFP-WIT1 was decreased by decreasing the OD_{600} of the infiltrated *Agrobacterium tumefaciens* culture to one-fifth or one-tenth of the value used for other experiments, the overall weaker WIT1 signal was now also found associated with the NE (Supplemental Fig. S1B).

To further define the nature of the WIT1 aggregates, colocalization experiments with a marker that labels the ER were performed (Nelson et al., 2007). WIT1 aggregates clearly colocalized with the ER marker (Fig. 2D, top). The ER marker by itself did not show any aggregate formation (data not shown), as described previously (Nelson et al., 2007). In some cells, WIT1 and the ER marker colocalized in a meshwork-like pattern, indicative of ER (Fig. 2D, bottom). This suggests that aggregates consist at least in part of WIT1-associated ER material.

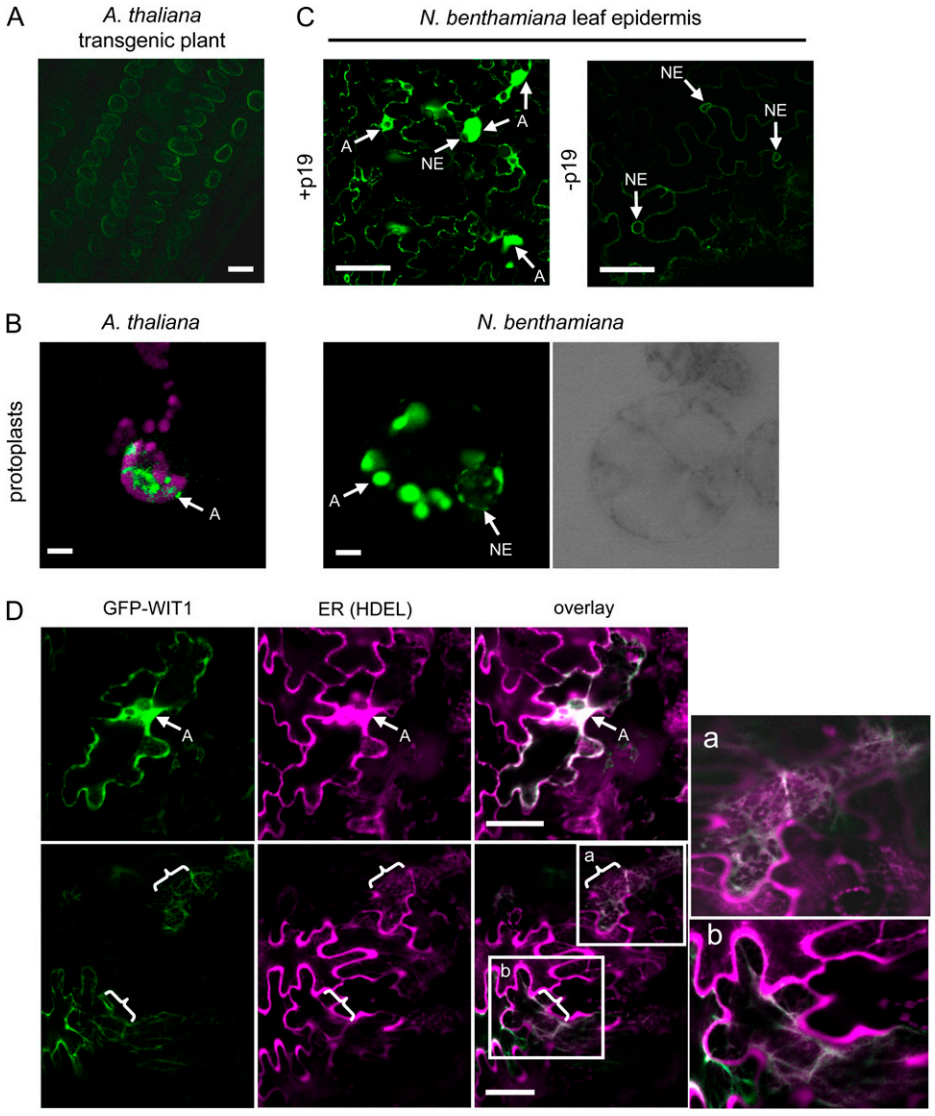

Figure 2. WIT1 forms aggregates when overexpressed. A, Root cells of a transgenic Arabidopsis line expressing 35S-driven GFP-WIT1. GFP-WIT1 expression was visualized in different transient expression systems (B and C). B, Transiently transformed leaf mesophyll Arabidopsis protoplasts (magenta signal, chlorophyll autofluorescence) and *N. benthamiana* protoplasts (latter is shown with corresponding bright-field image to mark the position of the nucleus). C, Agroinfiltrated *N. benthamiana* leaves (with or without p19). D, WIT1 colocalizes with an ER marker. *N. benthamiana* leaves were coagroinfiltrated with GFP-WIT1 (green) and an mCherry-HDEL ER marker (magenta; Nelson et al., 2007) in the presence of p19. Two magnified insets (a and b) were shown to enable better visualization of colocalization within the ER. A, Aggregation; braces, ER. Bars = 10 μm. The gain settings for images presented in A and C (right) were significantly higher than for other images for better visualization.

Coexpression of WPP1, WPP2, and HSC70-1 Prevents Formation of WIT1 Aggregates in *N. benthamiana*

Studies in animals suggest that membrane insertion of some TA proteins with very hydrophobic TMDs is assisted by chaperones, without which they form insoluble aggregates (Borgese et al., 2007). The Hsc70/Hsp40 chaperone complex was identified as one of the two ATP-dependent complexes that interact with mammalian TA protein substrates in vitro and assist in their delivery (Abell et al., 2007; Stefanovic and Hegde, 2007; Rabu et al., 2008). Because WIT1 and HSC70 had both been found in an in vivo complex with WPP1 and WPP2, we tested whether Arabidopsis HSC70-1 or HSC70-3 would prevent the cytoplasmic aggregation of WIT1. Since WPP-domain proteins interact with both WIT1 and HSC70-1/HSC70-3, we also tested their effect on WIT1 localization.

HA-tagged HSC70-1, HSC70-3, and WPP-domain proteins were coexpressed one by one with GFP-WIT1 in *N. benthamiana*. Coagroinfiltration of GFP-WIT1 with HSC70-1, WPP1, or WPP2 led to a significantly reduced number of WIT1 aggregates compared with GUS coexpression (Fig. 3A). In addition, the association of WIT1 with the NE could be detected when HSC70-1, WPP1, or WPP2 were coexpressed (Fig. 3A; Supplemental Fig. S4). The percentage of cells that contained aggregates decreased from about 73% in case of GUS coexpression, to 31%, 23%, and 17% for HSC70-1, WPP1, and WPP2 coexpression, respectively (Fig. 3B). In contrast, coexpression of HSC70-3 did not decrease WIT1 aggregation (Fig. 3, A and B; Supplemental Fig. S5). Immunoblot analysis showed that all HA-tagged proteins were expressed and that the level of GFP-WIT1 was comparable in all samples (Fig. 3C). Importantly, it was highest in the sample coexpressing

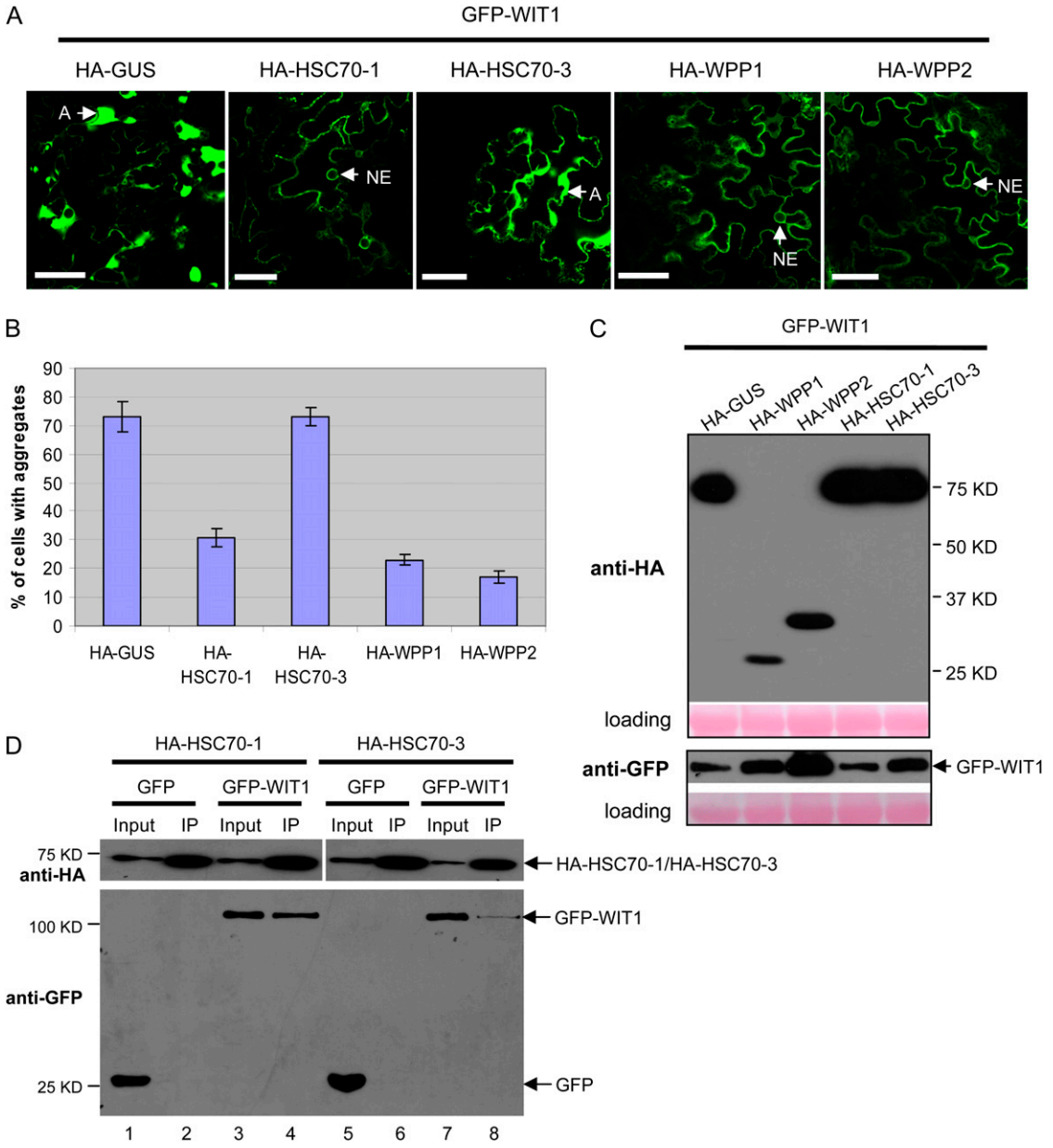

Figure 3. HSC70-1, WPP1, and WPP2 prevent GFP-WIT1 aggregates in *N. benthamiana*. A, GFP-WIT1 was coexpressed by coagroinfiltration in *N. benthamiana* leaves with one of the HA-tagged constructs: GUS, WPP1, WPP2, HSC70-1, and HSC70-3 and in the presence of p19. A, Aggregation. Bars = 10 μm. B, Quantification of aggregation in the coinfiltration experiment shown in A. The graph depicts the mean and SD values obtained from three independent experiments. A minimum of 200 cells total were scored for each agroinfiltrated combination. C, Anti-HA immunoblot of protein extracts from infiltrated leaves expressing GFP-WIT1 with the constructs as explained in A (top). Anti-GFP immunoblot showing comparable GFP-WIT1 expression levels in the same protein extracts (bottom). Ponceau S-stained membranes are shown below each blot to indicate equal loading. D, HA-HSC70-1 or HA-HSC70-3 was coexpressed with either GFP or GFP-WIT1 in *N. benthamiana* in the presence of p19. Immunoprecipitation was performed using the anti-HA antibody, and coimmunoprecipitated proteins were detected with the anti-GFP antibody. IP, Immunoprecipitate. [See online article for color version of this figure.]

WPP2, indicating that the reduced number of WIT1 aggregates observed for HSC70-1, WPP1, and WPP2 coexpression is not simply based on lower WIT1 expression levels. Cells showing GFP-WIT1 aggregation were viable, either when GFP-WIT1 was present alone or in combination with HA-GUS or HA-HSC70-3, judged by the staining of cell walls only with propidium iodide (Supplemental Fig. S6; data not shown).

To test if the different effects of HSC70-1 and HSC70-3 on the aggregates correlate with their ability to bind GFP-WIT1, samples from the coinfiltrated leaves were subjected to coimmunoprecipitation. Figure 3D shows

that when similar amounts of HSC70-1 and HSC70-3 were immunoprecipitated with the anti-HA antibody, significantly more GFP-WIT1 was detected in the precipitates with HSC70-1 than with HSC70-3 (compare lanes 4 and 8 in Fig. 3D). No signal was detected from leaves coexpressing free GFP. This result suggests higher stability of the complex containing WIT1 and HSC70-1 than the one containing WIT1 and HSC70-3, consistent with the observed effect on the GFP-WIT1 aggregates.

To also test the interaction of WIT1 with endogenous HSC70 in Arabidopsis, a coimmunoprecipitation using transgenic plants expressing GFP-WIT1 under the control of the 35S promoter was performed. As a control, a transgenic plant expressing 35S-driven GFP was used. Unlike GFP, which did not coimmunoprecipitate any HSC70, GFP-WIT1 bound significant amounts of endogenous HSC70 (Supplemental Fig. S7).

The Three-Amino-Acid WPP Motif of WPP1 Is Required to Prevent the GFP-WIT1 Aggregates

The conserved amino acid motif WPP in the WPP domain of RanGAP1 is critical for RanGAP1 binding to WIT1 (Zhao et al., 2008). The WPP domains of RanGAP1 and WPP1 show high sequence similarity and share the conserved WPP motif (Rose and Meier, 2001; Patel et al., 2004). A WPP to AAP mutation was introduced into WPP1, and the effect on the GFP-WIT1 aggregates was tested in *N. benthamiana*. While WPP1 largely prevented formation of GFP-WIT1 aggregates (as shown in Fig. 3), WPP1$^{WPP/AAP}$ failed to reduce WIT1 aggregates when the two proteins were coexpressed (Fig. 4A; Supplemental Fig. S8). The percentage of cells that contained aggregates when WPP1$^{WPP/AAP}$ was coinfiltrated was 77%, compared to 24% in the case of the wild-type protein and based on three independent experiments. Consistently, the interaction between WPP1$^{WPP/AAP}$ and WIT1 was largely reduced (Fig. 4B). We conclude that the effect of WPP1 on the GFP-WIT1 aggregates is specific and depends on the ability of two proteins to interact.

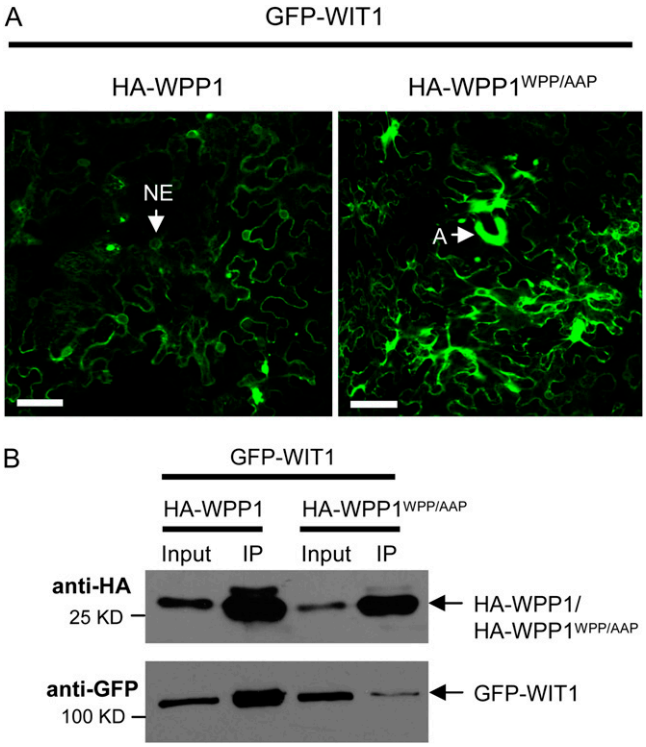

Figure 4. The three-amino-acid WPP motif of WPP1 is required to prevent the GFP-WIT1 aggregates. A, GFP-WIT1 was coexpressed with either HA-WPP1 or HA-WPP1$^{WPP/AAP}$ in *N. benthamiana* leaves by coagroinfiltration in the presence of p19. A, Aggregates. Bars = 10 μm. B, WPP1$^{WPP/AAP}$ has reduced affinity for WIT1. GFP-WIT1 was coexpressed with either HA-WPP1 or HA-WPP1$^{WPP/AAP}$ in *N. benthamiana* leaves by coagroinfiltration in the presence of p19. Immunoprecipitation was performed using the anti-HA antibody, and coimmunoprecipitated protein was detected with the anti-GFP antibody. The positions of proteins are depicted with arrows. IP, Immunoprecipitate. [See online article for color version of this figure.]

GFP-WIT1$^{1-660}$ Forms Aggregates That Are Prevented by WPP2 and HSC70-1

To test whether amino acids 1 to 660 of WIT1, containing the coiled-coil domain but lacking the TMD (Supplemental Fig. S9), would also form aggregates, GFP-WIT1$^{1-660}$ was expressed in *N. benthamiana*. When coexpressed alone or with the unrelated HA-GUS construct, GFP-WIT1$^{1-660}$ formed aggregates in the majority of cells. These aggregates differed from those formed by GFP-WIT1 in that they did not cause the ER marker to coaggregate, consistent with the absence of a TMD on this construct (data not shown). Nevertheless, coinfiltrated WPP2 and HSC70-1 also significantly reduced the number of GFP-WIT1$^{1-660}$ aggregates (Fig. 5A). Immunoblot analysis confirmed that all three HA-tagged proteins were expressed. The level of GFP-WIT1$^{1-660}$ was only slightly reduced when WPP2 or HSC70-1 was present, compared to GUS coexpression (Fig. 5B). WPP2 and HSC70-1 reduced the number of GFP-WIT1$^{1-660}$ aggregates to a similar degree (Fig. 5C). Immunoprecipitation with the anti-HA antibody showed that both HA-WPP2 and HA-HSC70-1 coimmunoprecipitated GFP-WIT1 and GFP-WIT1$^{1-660}$ equally well (Fig. 5E), indicating that both proteins bind to WIT1 in the absence of the C-terminal predicted TMD. Based on our data with other WPP-interacting coiled-coil proteins, binding between GFP-WIT1$^{1-660}$ and WPP2 most likely depends on the coiled-coil domain (Patel et al., 2004; Xu et al., 2007). This suggests that at least in case of the WPP-domain proteins, the aggregates are prevented by association of a WPP-domain protein with the long coiled-coil domain of WIT1.

Interestingly, while HSC70-1 prevented aggregate formation of GFP-WIT1$^{1-660}$, the number of cells with proper NE targeting of this construct was not increased, indicating that in *N. benthamiana* a factor that

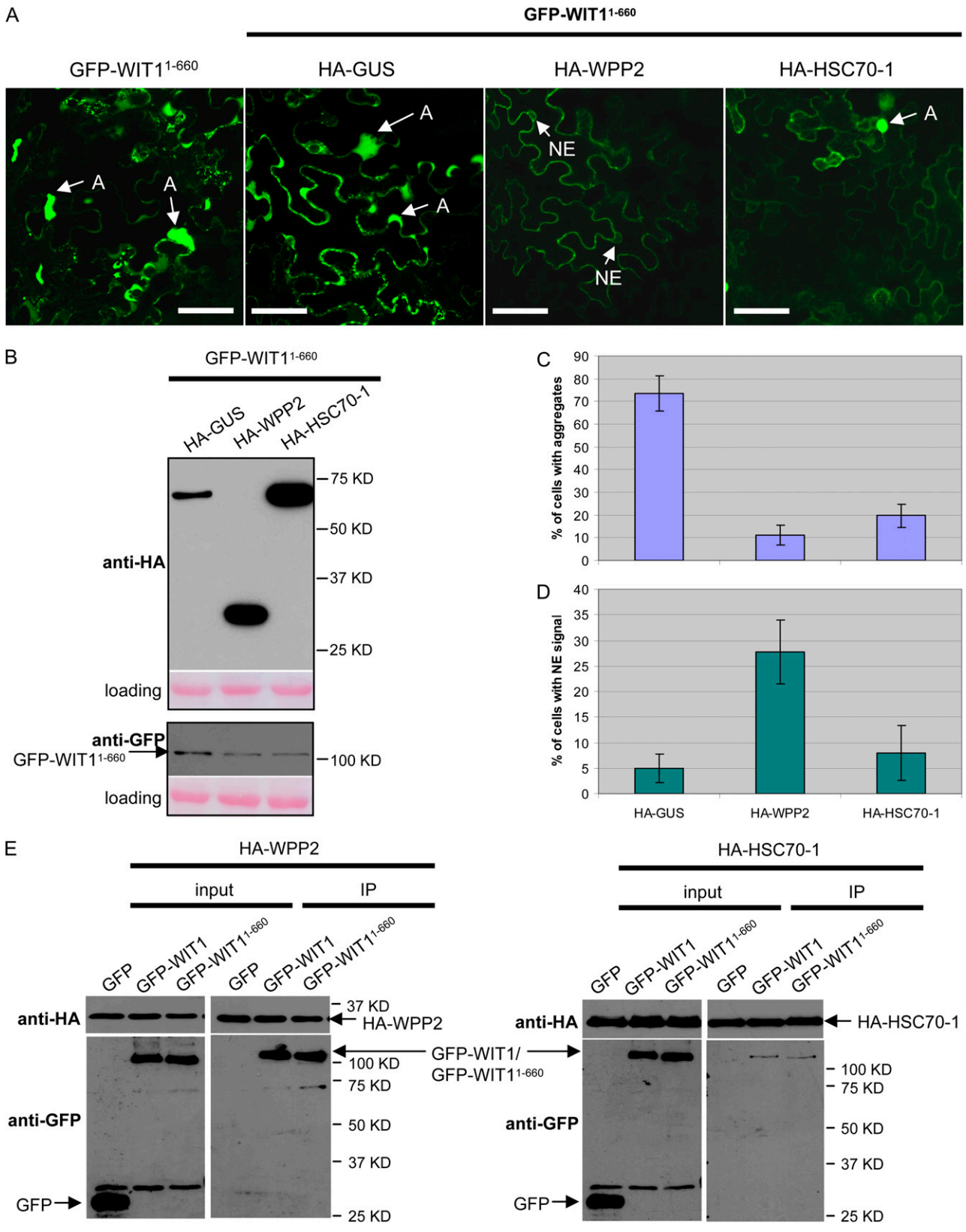

Figure 5. WPP2 and HSC70-1 decrease aggregation of WIT1$^{1-660}$ in *N. benthamiana*, and WPP2 promotes its NE-targeting. A, GFP-WIT1$^{1-660}$ was either expressed alone or coexpressed by coagroinfiltration in *N. benthamiana* leaves with one of the HA-tagged constructs: GUS, WPP2, and HSC70-1 in the presence of p19. A, Aggregation. Bars = 10 μm. B, Anti-HA immunoblot of

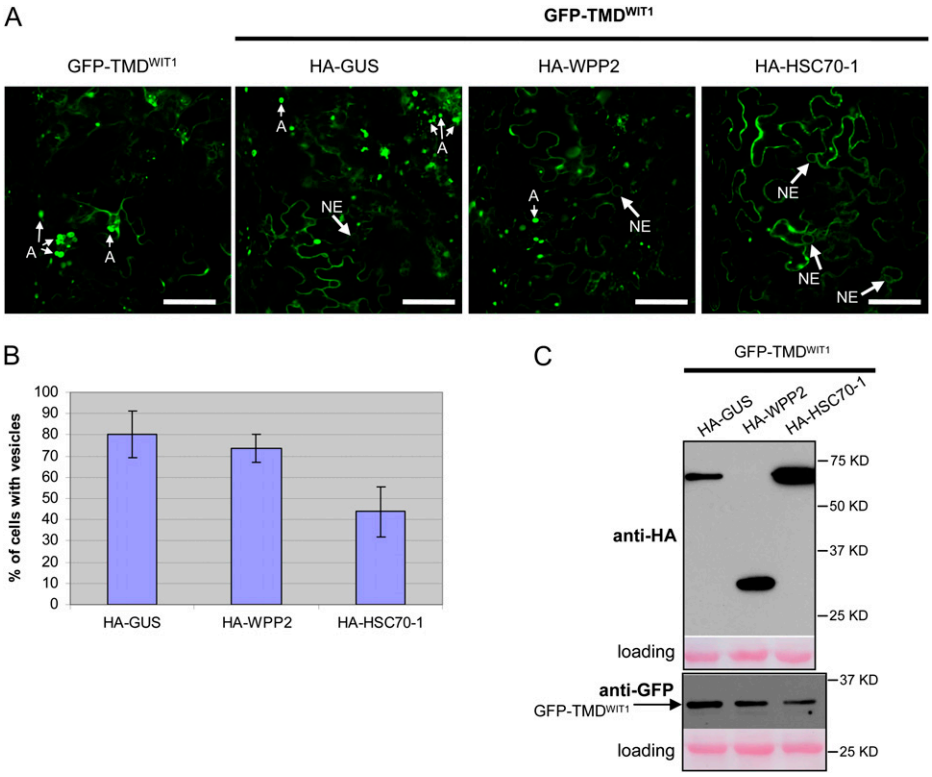

Figure 6. HSC70-1 decreases the number of aggregates formed in the presence of the tail region of WIT1 in *N. benthamiana*. A, GFP-TMD^{WIT1} was either expressed alone or coexpressed by coagroinfiltration in *N. benthamiana* leaves with one of the HA-tagged constructs: GUS, WPP2, and HSC70-1 in the presence of p19. A, Aggregates. Bars = 10 μm. B, Quantification of the number of aggregates present in the coinfiltration experiment shown in A. The graphs depict the mean and SD values obtained from two independent experiments. A minimum of 100 cells total were scored for each agroinfiltrated combination. C, Anti-HA immunoblot of protein extracts from infiltrated leaves expressing GFP-TMD^{WIT1} with the constructs as explained in A (top). Anti-GFP immunoblot showing comparable GFP-TMD^{WIT1} expression levels in the same protein extracts (bottom). Ponceau S-stained membranes are shown below each blot to indicate loading. [See online article for color version of this figure.]

is required for NE targeting of GFP-WIT1$^{1-660}$ might be missing, at least under the condition where both WIT1 and HSC70-1 are overexpressed. In contrast, HA-WPP2 coinfiltration not only reduced the number of aggregates but also increased the number of cells showing GFP-WIT1$^{1-660}$ at the NE (Fig. 5D), suggesting that WPP2 is involved in an additional step required for NE targeting in this background.

Only HSC70-1 Reduces the Number of Aggregates Formed by the C Terminus of WIT1

When expressed alone or with the GUS construct in *N. benthamiana*, GFP-TMD^{WIT1}, containing the very C-terminal 43 amino acids of WIT1, including the putative TMD (Supplemental Fig. S9), formed aggregates too, however, of a different shape (Fig. 6A; Supplemental Fig. S10). The aggregates were smaller, typically roundish, and sometimes appeared hollow. They were labeled by the ER marker (Supplemental Fig. S10), suggesting an ER membrane nature of the structures. Coexpression of HSC70-1 caused a decrease in the number of aggregates, while WPP2 had no significant effect (Fig. 6, A and B). Immunoblot analysis showed that all three HA-tagged proteins were expressed and that the expression level of GFP-TMD^{WIT1} was comparable in all three samples (Fig. 6C). This suggests that while HSC70-1 also acts somewhat to prevent aggregate formation of the WIT1 C terminus, WPP2 requires a domain within WIT1$^{1-660}$ for its activity.

WPP1, HSC70-1, and WIT1 Can Form a Ternary Complex

Since we have shown that WPP1 interacts with HSC70-1, WPP1 interacts with WIT1, and HSC70-1 interacts with WIT1, we asked if the three proteins are in the same complex. Therefore, HA-HSC70-1, WPP1-GFP, and FLAG-WIT1 were coinfiltrated in *N. benthamiana*, and as a control, GFP was coexpressed with

Figure 5. (*Continued.*)
protein extracts from infiltrated leaves expressing GFP-WIT1$^{1-660}$ with the constructs as explained in A (top). Anti-GFP immunoblot showing GFP-WIT1$^{1-660}$ expression levels in the same protein extracts (bottom). Ponceau S-stained membranes are shown below each blot to indicate equal loading. C and D, Quantification of aggregation (C) and NE targeting (D) in the coinfiltration experiment shown in A. The graphs depict the mean and SD values obtained from two independent experiments. A minimum of 100 cells total were scored for each agroinfiltrated combination. E, HA-WPP2 was coexpressed with either GFP, GFP-WIT1, or GFP-WIT1$^{1-660}$ (left); HA-HSC70-1 was coexpressed with either GFP, GFP-WIT1, or GFP-WIT1$^{1-660}$ (right) in *N. benthamiana* in the presence of p19. Immunoprecipitation was performed using the anti-HA antibody, and coimmunoprecipitated proteins were detected with the anti-GFP antibody. IP, Immunoprecipitate. [See online article for color version of this figure.]

HA-HSC70-1 and FLAG-WIT1. Samples were first immunoprecipitated with the anti-HA antibody. HA-HSC70-1 bound both WPP1-GFP and FLAG-WIT1, but not GFP (Fig. 7, HA-eluted). Then, anti-HA immunoprecipitated complexes were subjected to a second immunoprecipitation with the anti-GFP antibody. FLAG-WIT1 was only detected in the sample that contained WPP1-GFP (Fig. 7, GFP IP). These data show that WIT1 is simultaneously associated with both HSC70-1 and WPP1 and suggests that this ternary complex might be active in preventing the aggregates of WIT1.

DISCUSSION

WPP-Domain Proteins Interact with the Coiled-Coil Domain of WIT1

We have recently identified by tandem affinity purification coupled with mass spectrometry two NE-associated proteins, WIT1 and WIT2, which are required for RanGAP1 NE association in Arabidopsis root tip cells (Zhao et al., 2008). Here, we show that WIT1 also interacts in planta with two Arabidopsis proteins of unknown function that resemble the N-terminal domain of RanGAP proteins. WPP-domain proteins have previously been shown to interact with the coiled-coil domains of several proteins that also bind RanGAP1, including the Golgi-associated tomato (*Solanum lycopersicum*) protein LeWAP (Patel et al., 2005) and all three WIP family members (WIP1, WIP2a, and WIP3), which are also required for RanGAP1 NE targeting at the Arabidopsis root tip (Xu et al., 2007). RNA interference-based suppression of the Arabidopsis WPP family causes shorter primary roots, a reduced number of lateral roots, and reduced mitotic activity of the root meristem; however, the molecular function of WPP-domain proteins is not known (Patel et al., 2004). Here, we present evidence for a chaperone-like activity of WPP-domain proteins, reflected in preventing the aggregation of WIT1 and mediated by the interaction between WIT1 and WPP-domain proteins, likely through the coiled-coil domain of WIT1.

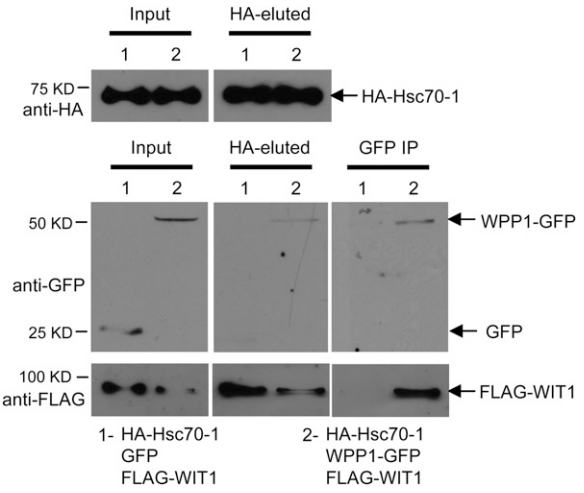

Figure 7. HSC70-1, WPP1, and WIT1 can be associated with the same complex in *N. benthamiana*. GFP-WIT1 was coexpressed with both HA-HSC70-1 and GFP (1) or with HA-HSC70-1 and WPP1-GFP (2) in *N. benthamiana* leaves by coagroinfiltration in the presence of p19. First immunoprecipitation was performed using the anti-HA antibody and immune complexes were eluted using HA peptide (HA-eluted). One-fifth of the HA-eluted sample was used for loading (HA-eluted). Second immunoprecipitation (IP) was performed using four-fifths of the HA-eluted fraction and the anti-GFP antibody. Coimmunoprecipitated protein was detected with the anti-FLAG antibody. The positions of proteins are depicted with arrows.

WIT1 Overexpression Aggregates Can Be Prevented by HSC70

As opposed to the specific NE localization detected for WIT1 in transgenic lines expressing GFP-WIT1 (Fig. 2A) and in wild-type Arabidopsis roots (Zhao et al., 2008), the majority of GFP-WIT1 was found in aggregates in *N. benthamiana*, in the presence of p19 (Fig. 2C). Both by omitting p19 from agroinfiltration and by decreasing the OD of the culture used for infiltration, WIT1 aggregation was significantly decreased and NE targeting supported (Fig. 2C; Supplemental Fig. S1B). Both aggregated and nonaggregated WIT1 colocalized with an ER marker, suggesting that WIT1 targeting to the NE includes the step of transit through the ER and that WIT1 aggregates form predominantly in close vicinity of the ER. Alternatively, WIT1 aggregates might represent correctly ER-inserted WIT1 that fails to fold properly, in which case targeting to the ER membrane is preserved, while further sorting from the ER to the NE is defective. This scenario is supported by the fact that the N terminus of WIT1 forms similar aggregates, but they do not colocalize with the ER. Here, we used the WIT1 aggregates as a tool to identify protein components required for the suppression of aggregation and for WIT1 and its deletion constructs to reach the NE.

We show that the Arabidopsis Hsc70 ortholog HSC70-1 can prevent Arabidopsis WIT1 from forming aggregates and promote its targeting to the NE in *N. benthamiana*. Unlike HSC70-1, HSC70-3 did not decrease WIT1 aggregation (Fig. 3A). Consistently, binding of WIT1 to HSC70-1 was significantly stronger than to HSC70-3 (Fig. 3D). The interaction of endogenous HSC70 with WIT1 was confirmed in Arabidopsis, using a transgenic line expressing GFP-WIT1. A recent report showed that the mammalian Hsc70 chaperone interacts with Sec61β, a TA protein, and is instrumental in its membrane insertion in vitro (Abell et al., 2007). Abell et al. (2007) have reconstituted the membrane integration of TA proteins using purified Hsc70. In addition, they found that a combination of Hsc70 and Hsp40 can completely substitute for the ATP-dependent factors present in the cytosol. In our case, Arabidopsis HSC70-1 may increase the solubility of WIT1 by inhibiting protein aggregation and therefore

keep WIT1 insertion-competent, as shown for yeast Hsc70 (Ngosuwan et al., 2003). In addition, it may represent a TMD-mediated targeting factor for WIT1, as suggested for mammalian Hsc70 (Abell et al., 2007).

WPP-Domain Proteins Mimic HSC70 in Preventing WIT1 Aggregation

Surprisingly, WPP1 and WPP2 were even more competent to decrease aggregation of WIT1 and facilitate its targeting to the NE than HSC70-1 (Fig. 3). Both WIT1 binding and the effect of WPP1 on the WIT1 aggregates required the three-amino-acid WPP motif (Fig. 4), suggesting that the latter requires specific protein-protein interaction. Interestingly, the overexpression of WPP1 or WPP2 was sufficient to cause this effect in the absence of overexpressed HSC70-1. This could either indicate that WPP-domain proteins interact with endogenous *N. benthamiana* HSC70 engaging in a ternary complex, similar to the one that formed when all three proteins were overexpressed (Fig. 7), or that they can function independently of HSC70 in preventing GFP-WIT1 aggregation.

WIT1 Domain Requirement for Subcellular Targeting and the Role of Chaperones

The tail region of WIT1, containing the putative TMD, also formed aggregates that colocalized with the ER but that were distinguishable by their round, more vesicle-like appearance. Unlike WPP2, which had no influence on the localization of this construct in *N. benthamiana*, HSC70-1 decreased the number of vesicle-like aggregates. It has been reported that several TA and non-TA proteins are able to bind to a component of the cytosolic TMD recognition complex in a TMD-dependent manner, suggesting that the TMD recognition complex-dependent pathway is not only utilized by more than one TA protein but under some circumstances also by substrates that ordinarily would use the SRP cotranslational pathway (Stefanovic and Hegde, 2007). The Hsc70-Hsp40 pathway is used by more than one TA protein as well (Abell et al., 2007). Current models suggest that the hydrophobicity of the TMD within a TA protein might determine which ATP-dependent targeting route a TA protein is going to utilize (Rabu et al., 2008).

The truncated WIT1$^{1\text{-}660}$ fragment that contains the coiled-coil domain (Supplemental Fig. S9) aggregated similarly to full-length WIT1 but did not colocalize with ER (Fig. 5). Both overexpressed WPP2 and HSC70-1 were able to prevent the aggregation of WIT1$^{1\text{-}660}$. In addition, WPP2 promoted NE targeting of the same truncated protein. When expressed in transgenic Arabidopsis, WIT1$^{1\text{-}660}$ showed clear NE association (Zhao et al., 2008), suggesting that the residues contained in this fragment are sufficient for NE targeting, most likely through protein-protein interactions. We propose that WPP-domain proteins represent cytoplasmic factors involved in the delivery/targeting of WIT1, acting by binding to the coiled-coil domain. The role of WPP-domain proteins in this scenario would primarily be to prevent the aggregation of the coiled-coil domain of WIT1 and to thereby enable correct protein-protein interactions. Interestingly, a majority of TA SNAREs and Golgins, proteins that also have long coiled-coil domains, require at least part of the coiled-coil domain, in addition to the TMD, for their proper membrane targeting (Linstedt et al., 1995; Kim et al., 1999; Misumi et al., 2001).

Besides WPP-domain proteins, WIT1 was also previously shown to interact with the WIP protein family, as well as with both RanGAP proteins (Zhao et al., 2008). Coexpression of WIT1 with WIP1 in *N. benthamiana* causes mislocalization of WIP1 from the NE and its relocation to the WIT1-like aggregates (data not shown). It is therefore likely that WIT1 aggregation in the absence of WPP proteins and HSC70 also leads to mistargeting of RanGAP and that WPP protein function is therefore indirectly important for proper RanGAP localization at the NE.

WPP-domain proteins have three important properties that allow us to propose their role as cytosolic chaperones/receptors for the posttranslational targeting of NE-localized protein(s). They specifically interact with the NE-localized, putative TA protein WIT1, they prevent its aggregation while increasing its NE targeting efficiency, and they are partly NE localized themselves. The proposed role of WPP-domain proteins may be analogous to that of PEX19, a protein with cytoplasmic/peroxisomal localization that binds to a number of peroxisomal membrane proteins (Sacksteder et al., 2000), including some TA proteins (Halbach et al., 2006), and plays a role of a chaperone/cytosolic receptor that targets peroxisomal membrane proteins to the peroxisomal membrane (Jones et al., 2004). Another example for a protein with a dual chaperone/receptor function is AKR2A, which is involved in the targeting of chloroplast outer envelope membrane proteins. In a manner very similar to the one we show here for the WPP-domain proteins, AKR2A prevents aggregation of its substrates, maintaining them in an insertion-competent form and increases their chloroplast targeting efficiency in vivo (Bae et al., 2008). Our data demonstrate that WPP1 and WPP2 are capable of interaction with HSC70, suggesting that WPP-domain proteins may cooperate with HSC70-1 in delivery/targeting of more than one substrate protein. Further studies are necessary to address whether targeting of other TA/coiled-coil domain-containing proteins can be assisted by WPP-domain proteins and if so, if WPP-domain proteins have a specific function for NE-localized proteins.

MATERIALS AND METHODS

Constructs

The *WPP1* gene was subcloned from pBD-GAL4 (Patel et al., 2004) to pENTR3C (Invitrogen) using the *Eco*RI restriction site. Cloning of the *WPP2*

gene into pENTR3C (Invitrogen) was described previously (Zhao et al., 2008). cDNAs of *HSC70-1* and *HSC70-3* (U09493 and U10908, respectively) were acquired from the Arabidopsis Biological Resource Center (The Ohio State University, Columbus, OH). Primers 5′-CACCATGTCGGGTAAAGGAGAAGGACC-3′ and 5′-TTAGTCGACCTCCTCGATCTTAGG-3′ were used to amplify the *HSC70-1* cDNA from the vector U09493 and insert it into pENTR/D-TOPO (Invitrogen). Primers 5′-CACCATGGCTGGTAAAGGAGAAGGTCC-3′ and 5′-TTAGTCGACTTCCTCAATCTTGGG-3′ were used to amplify the *HSC70-3* cDNA from the vector U10908 and insert it into pENTR/D-TOPO (Invitrogen). The inserts were confirmed by sequencing. The *WPP1*, *WPP1*$^{WPP/AAP}$, *WPP2*, *HSC70-1*, *HSC70-3*, and *GUS* (Invitrogen) cDNAs were moved into the HA-tag destination vector pEarleyGate201 (Early et al., 2006). The N-terminal TAP-WPP1 fusion construct was obtained by LR recombination (Invitrogen) with the NTAPi binary vector (Rohila et al., 2004). Constructs in pFGC5941 expressing GFP, WPP1-GFP, and WPP2-GFP (Patel et al., 2004), pK7WGF2 expressing GFP, GFP-WIT1, GFP-WIT1ΔTMD, and GFP-TMD^{WIT1}, NTAPi expressing WPP2, and pEarleyGate201 expressing FLAG-WIT1 (Zhao et al., 2008) were described previously. WPP1:WPP1-GFP and WPP2:WPP2-GFP in pFGC5941 were cloned as *Eco*RI/*Nco*I PCR fragments using primers 5′-GGAATTCCGATAATGTATTTTTATTGACCAATTC-3′ and 5′-CATGCCATGGAAGCTTCACTTGAATC-3′ for WPP1 and 5′-GGAATTCCTGTCCCATCTCCAACAAAA-3′ and 5′-CATGCCATGGAAGCCTCACTCTTC-3′ for WPP2, replacing the 35S promoter with a WPP1 genomic fragment containing promoter, 5′ untranslated region, and coding sequence of WPP1 (2016 bp) or with a WPP2 genomic fragment containing promoter, 5′ untranslated region, and coding sequence of WPP2 (2135 bp). The ER mCherry marker containing signal peptide of AtWAK2 and HDEL retention signal in pFGC19 (Nelson et al., 2007) was acquired from the Arabidopsis Biological Resource Center.

Site-Directed Mutagenesis

The conserved WPP motif in WPP1 was mutated to AAP using the mutagenic primer 5′-CATTTCCCTCAGAATCGCGGCACCGACTCAAAAAACTC-3′ and its complementary primer in pENTR3C (Invitrogen), using the QuikChange XL site-directed mutagenesis kit (Stratagene).

Generation of Transgenic Plants

The plasmid expressing TAP-WPP1 was mobilized into the *Agrobacterium tumefaciens* strain ABI. Transconjugants were selected on LB plates containing 50 μg/mL spectinomycin, 34 μg/mL chloramphenicol, and 50 μg/mL kanamycin. Plasmids expressing WPP1-GFP and WPP2-GFP under the control of their respective promoters were mobilized into the *A. tumefaciens* strain GV3101 by electroporation. Transformed agrobacteria were selected on LB plates containing 50 μg/mL kanamycin and 30 μg/mL gentamicin. Arabidopsis (*Arabidopsis thaliana*) ecotype Columbia wild-type plants were transformed by floral dipping (Clough and Bent, 1998) and selected for BASTA resistance. The generation of transgenic plants expressing TAP-WPP2 or GFP-WIT1 was described previously (Zhao et al., 2008).

Plant Cell Culture

Maintenance of *Nicotiana benthamiana* cell culture, isolation of protoplasts, and transformation by electroporation were performed as described (Zhong et al., 2005). Ten micrograms of GFP-WIT1 plasmid was used for electroporation, and localization of the expressed protein was tested by confocal microscopy after overnight incubation.

Arabidopsis Leaf Mesophyll Protoplast Isolation

The preparation of the leaf tissue, protoplast isolation, and polyethylene glycol transfection procedure was performed as described (Yoo et al., 2007). Twenty micrograms of GFP-WIT1 plasmid was used for transfection, and localization of the expressed protein was tested by confocal microscopy after 12 h of incubation.

Agroinfiltration in *N. benthamiana*

Plasmids expressing HA-WPP1, HA-WPP1$^{WPP/AAP}$, HA-WPP2, HA-HSC70-1, HA-HSC70-3, and HA-GUS were mobilized into the *A. tumefaciens* strain GV3101 by electroporation. Transformed agrobacteria were selected on LB plates containing 50 μg/mL kanamycin and 30 μg/mL gentamicin. *N. benthamiana* plants were grown in soil under standard long-day conditions (16 h light and 8 h dark) at 24°C for 3 weeks before agroinfiltration. *A. tumefaciens* cultures containing different plasmids were either infiltrated or coinfiltrated into *N. benthamiana* leaves as described previously (Zhao et al., 2006). The OD of each *A. tumefaciens* culture was 1.0 (unless indicated differently), and the ratio between each culture was 1:1 when two cultures were used for coinfiltration or 1:1:1 when three cultures were used for coinfiltration. Quantitative data were obtained by scoring two-dimensional fields of view. Ten to fifteen fields of view were scored per agroinfiltrated combination per experiment. Two to three replicates of each experiment were performed (as indicated in the legend of each figure). The gene silencing suppressor p19 (Voinnet et al., 2003) was coexpressed to prevent silencing from multiple 35S promoter-containing constructs, as was described previously (Zhao et al., 2006; Dixon et al., 2009). The presence or absence of p19 in each infiltration is specifically indicated in the figure legends.

Tandem Affinity Purification and Mass Spectrometry Analysis

Detailed description of TAP protocol and subsequent mass spectrometry analysis was given elsewhere (Zhao et al., 2008).

Immunoblot and Protein Interaction Analysis

Arabidopsis Columbia wild type expressing GFP or GFP-WIT1 (kanamycin resistant), GFP, WPP1-GFP, or WPP2-GFP (BASTA resistant), and TAP-WPP1 or TAP-WPP2 (BASTA resistant) were grown at 22°C in constant light for 14 d. *N. benthamiana* plants were grown for 3 d after agroinfiltration was performed. Whole Arabidopsis seedlings or infiltrated leaves of *N. benthamiana* were collected and ground into fine powders. Extracts for coimmunoprecipitation were prepared at 4°C in a buffer containing 50 mM Tris-HCl (pH 7.5), 150 mM NaCl, 0.5% NP-40, 1 mM EDTA, 3 mM dithiothreitol, 1 mM phenylmethylsulphonyl fluoride, and protease inhibitor cocktail (1:100; Sigma-Aldrich). Immunoprecipitates from both Arabidopsis and *N. benthamiana* were prepared either with monoclonal anti-GFP antibody (A11120; Molecular Probes), polyclonal anti-GFP antibody (ab290; Abcam), anti-WIT1 antibody (Zhao et al., 2008) bound to protein A-sepharose beads (GE Healthcare), or monoclonal anti-HA-agarose antibody produced in mouse (Sigma-Aldrich) with 1 to 2 h binding. The immunoprecipitates were then analyzed by SDS-PAGE, transferred to nitrocellulose or PVDF membranes, and probed with anti-WIT1 (1:2,000), mouse anti-Hsc70 (Hsp73) monoclonal antibody (1:1,000; Stressgen), monoclonal anti-HA-horseradish peroxidase (HRP; 1:5,000; Sigma-Aldrich), or anti-FLAG M2-HRP (1:1,000, Sigma-Aldrich) antibody. Two types of anti-GFP antibodies were used for detection of immunoprecipitates: polyclonal (A11122, 1:4,000; Molecular Probes) and monoclonal (MO48-3, 1:1,000; MBL). A dilution of 1:25,000 was used for the HRP-conjugated anti-rabbit secondary antibody (GE healthcare). HRP-conjugated anti-mouse secondary antibody (Sigma-Aldrich) was used as a dilution of 1:10,000. The loading ratio input: immunoprecipitation was 1:10 in each experiment, unless noted in the figure legend. For the Hsc70-1-WPP1-WIT1 ternary complex detection, extracts in immunoprecipitation buffer were first bound to anti-HA-agarose antibody (Sigma-Aldrich). After 1 h, bound proteins were eluted in five column volumes of immunoprecipitation buffer containing 100 μg/mL HA peptide (Sigma-Aldrich) for 15 min. Four-fifths of the eluate was bound to monoclonal anti-GFP antibody-protein A-sepharose beads, and after second immunoprecipitation, immune complexes were detected with anti-HA-HRP (1:5000; Sigma-Aldrich), anti GFP (A11122, 1:4,000; Molecular Probes), or anti-FLAG M2-HRP (1:1,000; Sigma-Aldrich) antibody. Each immunoprecipitation was repeated at least twice.

Confocal Microscopy

N. benthamiana was grown for 3 d after agroinfiltration. A small section was dissected from the infiltrated area and placed on a slide with coverslip for microscopy. The same section was used for immunoblotting to quantify the amount of proteins. GFP fluorescence images were collected on a PCM 2000/Nikon Eclipse E600 confocal laser scanning microscope as described (Rose and Meier, 2001).

Supplemental Data

The following materials are available in the online version of this article.

Supplemental Figure S1. GFP-WIT1 aggregation at different infiltration conditions.

Supplemental Figure S2. GFP-WIT1 aggregates do not form membrane whorls.

Supplemental Figure S3. GFP-WIT1 is localized at the NE in the absence of p19.

Supplemental Figure S4. GFP-WIT1 is localized at the NE when coexpressed with HA-WPP1.

Supplemental Figure S5. Unlike HSC70-3, HSC70-1 partially prevents GFP-WIT1 aggregation.

Supplemental Figure S6. Cells that contain GFP-WIT1 aggregates are viable.

Supplemental Figure S7. GFP-WIT1 binds to endogenous HSC70.

Supplemental Figure S8. $WPP1^{WPP/AAP}$ does not prevent GFP-WIT1 aggregation.

Supplemental Figure S9. Domain structure of WIT1 and WIT1 deletion constructs.

Supplemental Figure S10. The C terminus of WIT1 colocalizes with ER.

Supplemental Table S1. List of peptides identified in TAP-WPP1 LC/MS/MS analysis, corresponding to HSC70.

Supplemental Table S2. List of peptides identified in TAP-WPP2 LC/MS/MS analysis, corresponding to HSC70.

ACKNOWLEDGMENTS

We thank Xiao Zhou for help with the WIT1 domain localization experiments, Dr. Jyan-Chyun Jang for Arabidopsis leaf mesophyll protoplast isolation, Dr. Biao Ding for generous user time at his confocal microscope, and all members of the Meier lab for fruitful discussions.

Received June 22, 2009; accepted July 14, 2009; published July 17, 2009.

LITERATURE CITED

Abell BM, Rabu C, Leznicki P, Young JC, High S (2007) Post-translational integration of tail-anchored proteins is facilitated by defined molecular chaperones. J Cell Sci **120:** 1743–1751

Bae W, Lee YJ, Kim DH, Lee J, Kim S, Sohn EJ, Hwang I (2008) AKR2A-mediated import of chloroplast outer membrane proteins is essential for chloroplast biogenesis. Nat Cell Biol **10:** 220–227

Borgese N, Brambillasca S, Colombo S (2007) How tails guide tail-anchored proteins to their destinations. Curr Opin Cell Biol **19:** 368–375

Borgese N, Colombo S, Pedrazzini E (2003) The tale of tail-anchored proteins: coming from the cytosol and looking for a membrane. J Cell Biol **161:** 1013–1019

Bukau B, Horwich AL (1998) The Hsp70 and Hsp60 chaperone machines. Cell **92:** 351–366

Chirico WJ, Waters MG, Blobel G (1988) 70K heat shock related proteins stimulate protein translocation into microsomes. Nature **332:** 805–810

Clough SJ, Bent AF (1998) Floral dip: a simplified method for Agrobacterium-mediated transformation of *Arabidopsis thaliana*. Plant J **16:** 735–743

Deshaies RJ, Koch BD, Werner-Washburne M, Craig EA, Schekman R (1988) A subfamily of stress proteins facilitates translocation of secretory and mitochondrial precursor polypeptides. Nature **332:** 800–805

Dixon DP, Hawkins T, Hussey PJ, Edwards R (2009) Enzyme activities and subcellular localization of members of the Arabidopsis glutathione transferase superfamily. J Exp Bot **60:** 1207–1218

Dufresne PJ, Thivierge K, Cotton S, Beauchemin C, Ide C, Ubalijoro E, Laliberte JF, Fortin MG (2008) Heat shock 70 protein interaction with Turnip mosaic virus RNA-dependent RNA polymerase within virus-induced membrane vesicles. Virology **374:** 217–227

Early KW, Haag JR, Pontes O, Opper K, Juehne T, Song K, Pikaard CS (2006) Gateway-compatible vectors for plant functional genomics and proteomics. Plant J **45:** 616–629

Halbach A, Landgraf C, Lorenzen S, Rosenkranz K, Volkmer-Engert R, Erdmann R, Rottensteiner H (2006) Targeting of the tail-anchored peroxisomal membrane proteins PEX26 and PEX15 occurs through C-terminal PEX19-binding sites. J Cell Sci **119:** 2508–2517

Jones JM, Morrell JC, Gould SJ (2004) PEX19 is a predominantly cytosolic chaperone and import receptor for class 1 peroxisomal membrane proteins. J Cell Biol **164:** 57–67

Kim PK, Hollerbach C, Trimble WS, Leber B, Andrews DW (1999) Identification of the endoplasmic reticulum targeting signal in vesicle-associated membrane proteins. J Biol Chem **274:** 36876–36882

Linstedt AD, Foguet M, Renz M, Seelig HP, Glick BS, Hauri HP (1995) A C-terminally-anchored Golgi protein is inserted into the endoplasmic reticulum and then transported to the Golgi apparatus. Proc Natl Acad Sci USA **92:** 5102–5105

Matunis MJ, Coutavas E, Blobel G (1996) A novel ubiquitin-like modification modulates the partitioning of the Ran-GTPase-activating protein RanGAP1 between the cytosol and the nuclear pore complex. J Cell Biol **135:** 1457–1470

Meacham GC, Patterson C, Zhang W, Younger JM, Cyr DM (2001) The Hsc70 co-chaperone CHIP targets immature CFTR for proteasomal degradation. Nat Cell Biol **3:** 100–105

Misumi Y, Sohda M, Tashiro A, Sato H, Ikehara Y (2001) An essential cytoplasmic domain for the Golgi localization of coiled-coil proteins with a COOH-terminal membrane anchor. J Biol Chem **276:** 6867–6873

Nelson BK, Cai X, Nebenfuhr A (2007) A multicolored set of in vivo organelle markers for co-localization studies in Arabidopsis and other plants. Plant J **51:** 1126–1136

Ngosuwan J, Wang NM, Fung KL, Chirico WJ (2003) Roles of cytosolic Hsp70 and Hsp40 molecular chaperones in post-translational translocation of presecretory proteins into the endoplasmic reticulum. J Biol Chem **278:** 7034–7042

Noel LD, Cagna G, Stuttmann J, Wirthmuller L, Betsuyaku S, Witte CP, Bhat R, Pochon N, Colby T, Parker JE (2007) Interaction between SGT1 and cytosolic/nuclear HSC70 chaperones regulates Arabidopsis immune responses. Plant Cell **19:** 4061–4076

Patel S, Brkljacic J, Gindullis F, Rose A, Meier I (2005) The plant nuclear envelope protein MAF1 has an additional location at the Golgi and binds to a novel Golgi-associated coiled-coil protein. Planta **222:** 1028–1040

Patel S, Rose A, Meulia T, Dixit R, Cyr RJ, Meier I (2004) Arabidopsis WPP-domain proteins are developmentally associated with the nuclear envelope and promote cell division. Plant Cell **16:** 3260–3273

Rabu C, Wipf P, Brodsky JL, High S (2008) A precursor-specific role for Hsp40/Hsc70 during tail-anchored protein integration at the endoplasmic reticulum. J Biol Chem **283:** 27504–27513

Rohila JS, Chen M, Cerny R, Fromm ME (2004) Improved tandem affinity purification tag and methods for isolation of protein heterocomplexes from plants. Plant J **38:** 172–181

Rose A, Meier I (2001) A domain unique to plant RanGAP is responsible for its targeting to the plant nuclear rim. Proc Natl Acad Sci USA **98:** 15377–15382

Sacksteder KA, Jones JM, South ST, Li X, Liu Y, Gould SJ (2000) PEX19 binds multiple peroxisomal membrane proteins, is predominantly cytoplasmic, and is required for peroxisome membrane synthesis. J Cell Biol **148:** 931–944

Stefanovic S, Hegde RS (2007) Identification of a targeting factor for posttranslational membrane protein insertion into the ER. Cell **128:** 1147–1159

Sung DY, Guy CL (2003) Physiological and molecular assessment of altered expression of Hsc70-1 in Arabidopsis. Evidence for pleiotropic consequences. Plant Physiol **132:** 979–987

Sung DY, Vierling E, Guy CL (2001) Comprehensive expression profile analysis of the Arabidopsis Hsp70 gene family. Plant Physiol **126:** 789–800

Voinnet O, Rivas S, Mestre P, Baulcombe D (2003) An enhanced transient expression system in plants based on suppression of gene silencing by the p19 protein of tomato bushy stunt virus. Plant J **33:** 949–956

Xu XM, Meulia T, Meier I (2007) Anchorage of plant RanGAP to the nuclear envelope involves novel nuclear-pore-associated proteins. Curr Biol **17:** 1157–1163

Yoo SD, Cho YH, Sheen J (2007) Arabidopsis mesophyll protoplasts: a versatile cell system for transient gene expression analysis. Nat Protocols **2:** 1565–1572

Zhang C, Guy CL (2005) Co-immunoprecipitation of Hsp101 with cytosolic Hsc70. Plant Physiol Biochem **43:** 13–18

Zhao Q, Brkljacic J, Meier I (2008) Two distinct interacting classes of nuclear envelope-associated coiled-coil proteins are required for the tissue-specific nuclear envelope targeting of *Arabidopsis* RanGAP. Plant Cell **20:** 1639–1651

Zhao Q, Leung S, Corbett AH, Meier I (2006) Identification and characterization of the Arabidopsis orthologs of nuclear transport factor 2, the nuclear import factor of ran. Plant Physiol **140:** 869–878

Zhong X, Itaya A, Ding B (2005) Transfecting protoplasts by electroporation to study viroid replication. Curr Protoc Microbiol **Chapter 16:** Unit 16D.4